

Engineering Notes

ENGINEERING NOTES are short manuscripts describing new developments or important results of a preliminary nature. These Notes should not exceed 2500 words (where a figure or table counts as 200 words). Following informal review by the Editors, they may be published within a few months of the date of receipt. Style requirements are the same as for regular contributions (see inside back cover).

Unpowered Approach and Landing Guidance with Normal Acceleration Limitations

C. A. Kluever*

University of Missouri–Columbia,
Columbia, Missouri 65211

DOI: 10.2514/1.28081

Introduction

FUTURE reusable launch vehicles (RLV) may greatly benefit from advanced guidance and control (AG&C) technologies. Hanson [1–3] has argued that AG&C will greatly improve safety and reliability by successfully returning an RLV that is plagued by aerosurface failures, poor vehicle performance, and larger-than-expected flight dispersions. Advanced guidance methods have been developed for the ascent, entry, and landing phases of an RLV [3–10].

Approach and landing (A&L) is a critical flight phase that brings the unpowered vehicle from the terminal area energy management (TAEM) phase to runway touchdown. The Space Shuttle A&L guidance scheme uses a two-phase (steep and shallow) reference flight path, which has proven to be effective for low lift-to-drag (L/D) vehicles [11]. Shuttle guidance also relies on a small set of fixed A&L reference profiles, and therefore it may not be well-suited for scenarios with large trajectory dispersions, poor vehicle performance, or actuator failures. Schierman et al. [9] and Kluever [10] have developed onboard trajectory-resaping algorithms for the A&L phase of an RLV. Both algorithms recompute a new reference A&L path in the presence of winds, aerodynamic uncertainties, and extreme trajectory dispersions.

This Note presents an A&L guidance scheme for an unpowered vehicle with diminished maneuverability in the vertical plane, namely, limited normal acceleration capabilities. An RLV with limited normal acceleration will have difficulty transitioning from the initial steep glide slope to a shallow flight path required for touchdown. The proposed guidance method computes a new reference trajectory such that load factor is minimized during the A&L phase. Trajectory planning is accomplished by performing a series of 1-D searches by iterating on a single guidance parameter and numerically propagating multiple paths to touchdown conditions. Numerical results are presented to demonstrate the effectiveness of the guidance method.

Received 28 September 2006; revision received 7 December 2006; accepted for publication 7 December 2006. Copyright © 2007 by the American Institute of Aeronautics and Astronautics, Inc. All rights reserved. Copies of this paper may be made for personal or internal use, on condition that the copier pay the \$10.00 per-copy fee to the Copyright Clearance Center, Inc., 222 Rosewood Drive, Danvers, MA 01923; include the code 0731-5090/07 \$10.00 in correspondence with the CCC.

*Professor, Mechanical and Aerospace Engineering Department, Associate Fellow AIAA.

System Models

Equations of Motion

The unpowered RLV is considered as a point mass, and its gliding motion in a vertical plane is defined by

$$\dot{V} = \frac{-D}{m} - g \sin \gamma \quad (1)$$

$$\dot{\gamma} = \frac{L}{mV} - \frac{g}{V} \cos \gamma \quad (2)$$

$$\dot{h} = V \sin \gamma \quad (3)$$

$$\dot{x} = V \cos \gamma \quad (4)$$

where V is the airspeed, γ is the flight-path angle, h is the altitude, x is the downtrack position along the runway centerline, m is the mass, and g is the Earth's gravitational acceleration. Lift and drag forces are defined in the usual manner:

$$L = \bar{q} S C_L \quad D = \bar{q} S C_D \quad (5)$$

where C_L and C_D are lift and drag coefficients, S is the reference area, and dynamic pressure is $\bar{q} = \rho V^2/2$. The governing equations of motion (1–4) are with respect to a “flat-Earth” model, where the $+x$ axis points along the runway centerline, with the origin at the runway threshold. Atmospheric density ρ is computed using the Standard Atmosphere.

Vehicle Models

The X-33 is the test vehicle for guidance algorithm development, and it was used here due to the availability of aerodynamic data and its extensive use as a test vehicle for the AG&C Program. Reference area is $S = 1607.8 \text{ ft}^2$ and mass is $83,000 \text{ lb}_m$ (2579.7 slugs). Lift and drag aerodynamic coefficients are computed by a 2-D table lookup with angle of attack α and Mach number M as the independent variables:

$$C_L = C_L(\alpha, M) \quad C_D = C_D(\alpha, M) \quad (6)$$

Incremental changes in lift and drag coefficients due to ground effects are also computed by a 2-D table lookup with altitude above the runway and angle of attack as the input variables.

Our prior guidance development work for TAEM and A&L relied on an approximate model of the X-33 aerodynamics for onboard trajectory generation [10,12], and a similar approach is taken in this work. A standard drag polar is used to model the X-33 aerodynamics:

$$C_D = C_{D0} + K C_L^N \quad (7)$$

Zero-lift drag coefficient C_{D0} , lift-induced drag coefficient parameter K , and exponent N are obtained by fitting the drag polar (7) to the “true” aerodynamic data from the 2-D lookup tables. Kluever [10] presents the numerical details for these values over a Mach number range from 0.6 to 0.3.

Approach and Landing Guidance

Because the X-33 has a maximum L/D ratio around 3.5, it must initially follow a fairly steep glide slope. Kluever [10] shows that the steep glide slope ($\gamma = -25^\circ$) is followed by a circular pullup maneuver at an altitude of about 2200 ft, which requires a sustained normal acceleration of about 1.3g for about 15 s, with a peak normal acceleration greater than 1.4g. An RLV with load factor limitations may not be able to generate or sustain normal accelerations at this level during a pullup maneuver.

Optimization Trials

Quantifying the appropriate limitations for normal acceleration proved to be a challenging task. Initially, it was not clear which vertical parameter should be constrained, and therefore a series of optimization trials were performed. A&L trajectory optimization was performed by using an inverse-dynamics approach, where parameters defining the flight-path angle profile $\gamma(x)$ served as free optimization variables, and the control (lift coefficient) required to track the flight path was computed from the governing dynamics (2). Constraints were imposed on the touchdown conditions (sink rate and airspeed), and the parameter optimization problem was solved using sequential quadratic programming (see [12] for details of the optimization approach as applied to the TAEM trajectory problem).

The optimization trials will be briefly summarized. Initially, we minimized the summation of incremental changes in α squared, or $\sum (\alpha_{i+1} - \alpha_i)^2$, where α_i is angle of attack evaluated at each discrete step of the trajectory solution. Therefore, an A&L trajectory with a constant angle of attack would provide the absolute minimum. Although this optimization trial produced an A&L trajectory where the α range was small (3.5–6.5 deg), the initial glide slope was very steep ($\gamma = -47^\circ$), and the vehicle experienced high airspeed and high normal acceleration ($> 1.5g$) during the pullup maneuver before touchdown. This optimization trial did not seem to best represent a vehicle with limited normal acceleration.

Next, minimizing the integral of load factor was investigated. The “equilibrium-glide load factor” is defined as

$$n_{EG} = \frac{L}{mg \cos \gamma} \quad (8)$$

Solving Eq. (8) for lift L and substituting into Eq. (2) results in

$$\dot{\gamma} = \frac{g \cos \gamma}{V} (n_{EG} - 1) \quad (9)$$

Hence, if $n_{EG} = 1$, the RLV will follow an “equilibrium glide” with constant flight-path angle. Clearly, n_{EG} must eventually exceed unity during A&L to rotate the flight-path angle upward and arrest sink rate before touchdown. The second optimization trial minimized the integral of $(n_{EG} - 1)^2$, which represents the sum of squared variations from the equilibrium glide condition. The solution to this optimization problem results in equilibrium glide ($n_{EG} = 1$) during the majority of A&L (i.e., a steep glide slope), followed by a sustained pullup and flare with n_{EG} at about 1.3g. This optimization trial also did not seem to best represent a vehicle with limited normal acceleration.

The third optimization trial minimized the peak value of n_{EG} , and its solution resulted in a constant load factor $n_{EG} = 1.1g$ during the entire A&L trajectory. Therefore, the RLV applies a small, constant normal acceleration component (in excess of what is needed for equilibrium glide) to continuously rotate the flight-path angle upward. The result of this optimization trial seems to best represent an unpowered vehicle with load factor limitations, and therefore a guidance scheme for this type of A&L trajectory was developed. From an operational standpoint, an aerosurface actuator failure would degrade the vertical maneuverability of the RLV, in which case the minimum load factor guidance would be used to control the flight path.

Path-Planning Algorithm

The path-planning algorithm attempts to mimic the results from the third optimization trial by determining the minimum constant n_{EG} that produces the desired states at touchdown. Propagating multiple A&L paths is required, and this task is performed by numerically integrating the governing equations with energy height E as the independent variable. Energy height is total mechanical energy divided by weight, $E = V^2/2g + h$, and its time-rate of change is

$$\dot{E} = \frac{-DV}{mg} \quad (10)$$

Equations (9), (3), and (4) can be divided by Eq. (10) to produce the governing equations $d\gamma/dE$, dh/dE , and dx/dE , which can be integrated between fixed boundary conditions for E . Approach and landing interface (ALI) is the transition from TAEM to A&L, and it is defined as the point where the vehicle reaches a runway altitude of 10,000 ft. The desired touchdown airspeed is fixed at 273.7 ft/s, which corresponds to an energy reserve of 6 s (energy reserve is the difference between touchdown and stall airspeeds divided by deceleration at touchdown), and therefore $E = 1164$ ft at touchdown. The unknown parameters required for propagating the A&L trajectory are flight-path angle at ALI (γ_{ALI}), airspeed at ALI (V_{ALI}), and constant load factor n_{EG} . Terminal trajectory constraints at touchdown are $h_{TD} = 0$ and sink rate $-5 \leq \dot{h}_{TD} \leq -2$ ft/s. Selecting V_{ALI} determines the initial energy height (E_{ALI}), and enforcing the terminal altitude constraint after integrating dh/dE ensures the proper airspeed at touchdown because E_{TD} is fixed at 1164 ft. Lift coefficient C_L is determined from Eq. (8) by using a trial (constant) load factor n_{EG} , and C_D is computed from the approximate drag polar (7). Airspeed is needed during the numerical integration (for dynamic pressure), and it is computed from energy E and altitude h . Numerical integration is performed by a first-order Euler method with 50 fixed-size steps in energy height. The A&L profiles for flight-path angle, altitude, and downtrack distance are all monotonic when n_{EG} is constant, and therefore Euler integration is sufficiently accurate as well as computationally inexpensive.

The onboard trajectory-planning algorithm can now be summarized: a desired value of V_{ALI} is selected (this may be known during the latter stages of TAEM), and a trial value for n_{EG} is selected. Next, a 1-D search is performed to determine the initial flight-path angle (γ_{ALI}) such that the propagated terminal altitude equals zero. A Newton iteration is used to adjust γ_{ALI}

$$\Delta h_{TD} = \frac{\partial h_{TD}}{\partial \gamma_{ALI}} \Delta \gamma_{ALI} \quad (11)$$

where the partial derivative is computed using finite-difference methods and a neighboring trajectory. This first-order gradient search typically converges in four or five iterations (convergence is defined by $|h_{TD}| \leq 0.01$ ft). After convergence on altitude is achieved, the sink rate at touchdown is checked, and if its magnitude is less than 5 ft/s, the trajectory-planning problem has been solved. If sink-rate magnitude is too great (i.e., $\dot{h}_{TD} < -5$ ft/s), then the constant load factor n_{EG} is increased and the process is continued until the touchdown sink rate has been properly arrested. This trajectory-planning scheme is robust for two reasons: 1) satisfying the altitude constraint $h_{TD} = 0$ by iterating on γ_{ALI} is relatively easy and converges quickly, and 2) starting the load factor iteration loop with a value slightly greater than unity (e.g., $n_{EG} = 1.002g$) will produce an A&L path with very little curvature such that the touchdown sink rate is a large negative value. Therefore, the minimum value for n_{EG} can be obtained by starting the search “from below” and stopping when a feasible A&L path is found.

Numerical Results

Several reference A&L paths are obtained for ALI airspeed ranging from 350 to 650 ft/s. Because ALI altitude is 10,000 ft, these minimum and maximum values of V_{ALI} approach the lower and upper boundaries on dynamic pressure for the X-33. The trajectory-

Table 1 Initial energy variation trials with trajectory-planning algorithm^a

V_{ALI} , ft/s	n_{EG} , g	γ_{ALI} , deg	x_{ALI} , ft	V_{TD} , ft/s	\dot{h}_{TD} , ft/s	x_{TD} , ft	avg n_{EG} , g	max n_{EG} , g
350	1.104	-33.71	-26,585	268.4	-5.1	1660	1.100	1.171
400	1.102	-32.17	-27,119	268.8	-5.5	1660	1.098	1.173
450	1.102	-31.04	-27,545	268.4	-5.0	1687	1.097	1.168
500	1.100	-29.83	-28,088	268.6	-5.4	1689	1.095	1.169
550	1.100	-28.95	-28,516	268.2	-4.9	1718	1.095	1.166
600	1.098	-27.96	-29,054	268.8	-5.4	1714	1.093	1.168
650	1.098	-27.24	-29,472	268.8	-4.9	1743	1.092	1.166

^aTarget states at touchdown: $V_{\text{TD}} = 273.7$ ft/s, $\dot{h}_{\text{TD}} = -5$ ft/s, $x_{\text{TD}} = 1400$ ft.

planning algorithm described in the preceding section readily obtained a new reference A&L trajectory with minimum n_{EG} for all initial airspeeds. Normal acceleration n_{EG} was incremented by $0.002g$ in the outer loop of the two-stage iteration method for the trajectory-planning algorithm.

The accuracy of each minimum- n_{EG} path was demonstrated by executing a Simulink® simulation of the RLV dynamics (1–4), which uses the complete 2-D aerodynamic database (6) and a variable-step, second/third-order numerical integration method with a maximum step size of 0.1 s. The Simulink A&L simulation uses acceleration along the negative z -body axis (n_z) as the vertical guidance command, which consists of open- and closed-loop terms. Open-loop n_z command is computed from C_L , C_D , and α , where C_L is computed from the reference n_{EG} command and the current flight-path angle [see Eq. (8)]. A simple proportional-integral-derivative (PID) scheme is used for the closed-loop Δn_z term:

$$\Delta n_z = K_P \Delta h + K_I \int \Delta h dt + K_D \Delta \dot{h} \quad (12)$$

where $\Delta h = h_{\text{ref}} - h$ and $\Delta \dot{h} = \dot{h}_{\text{ref}} - \dot{h}$. The reference altitude and sink rate are determined by using the stored functions $h_{\text{ref}}(x)$ and $\dot{h}_{\text{ref}}(x)$ from the trajectory-planning results. The PID gains used here are $K_P = 0.004$ g/ft, $K_I = 0.00016$ g/ft · s, and $K_D = 0.024$ g · s/ft, which are similar to the Shuttle's gains for A&L. An approximate model for longitudinal pitching motion is also included in the Simulink simulation (see [10] for further details regarding the A&L simulation).

Table 1 summarizes the results from the trajectory-planning algorithm and the subsequent closed-loop A&L simulation using the Simulink model. Columns 2–4 in Table 1 present the constant load factor n_{EG} , ALI flight-path angle, and downtrack ALI location that are determined by the trajectory-planning algorithm and its two-stage iteration method. Recall that the trajectory-planning algorithm propagates three dynamical equations with respect to energy and uses a fixed-step Euler method for numerical integration. Although minimum n_{EG} is essentially $1.1g$ for the entire range of initial energy

configurations, normal acceleration decreases slightly for higher initial airspeeds (recall that the normal acceleration optimization problem also resulted in $n_{\text{EG}} = 1.1g$). Note also that initial flight-path angle (γ_{ALI}) becomes steeper as V_{ALI} decreases, and ALI downtrack position (x_{ALI}) moves farther from the runway threshold as V_{ALI} increases. Columns 5–9 present results from the Simulink simulation with the full aerodynamic model and a closed-loop guidance scheme that attempts to track the A&L reference path from the trajectory-planning algorithm. Note that touchdown airspeed V_{TD} and touchdown sink rate \dot{h}_{TD} are consistent for the range of initial airspeeds and A&L reference paths and show a very good match with their respective target values. Downtrack touchdown location overshoots the target value by about 300 ft, and this slight error could be alleviated by a more thorough guidance law design for a final flare maneuver. Average normal acceleration from the closed-loop simulation is slightly less than the open-loop (constant) command. All seven trials show a maximum (peak) n_{EG} value that is 6% greater than the open-loop n_{EG} command. This small $0.07g$ spike in normal acceleration occurs at an altitude of about 40 ft and typically lasts for 1–2 s, and is likely attributed to an increase in lift from ground effects, which are not modeled in the trajectory-planning algorithm.

Figure 1 shows flight-path angle vs downtrack position for two sets of A&L trajectories, where initial airspeed is $V_{\text{ALI}} = 350, 450, 550$, and 650 ft/s, respectively. Reshaped trajectories using a minimum- n_{EG} profile show a steady positive rotation of the flight-path angle. Because the rate $d\gamma/dx$ is inversely proportional to V^2 [divide Eq. (9) by Eq. (4)], this slope steadily increases as airspeed decreases along the A&L path because n_{EG} remains constant. Note that all four minimum- n_{EG} trajectories converge to the same A&L path as the RLV approaches touchdown. Trajectories using a fixed A&L reference with a $1.1g$ load factor limit are also shown in Fig. 1 for comparison (the reference path is the nominal A&L case from [10]). These trajectories all start at the same downtrack position ($x_{\text{ALI}} = -26,316$ ft) and initially maintain a fixed steep glide slope ($\gamma = -25.2$ deg) until the pullup altitude is reached (at about 10,000 ft ahead of the runway threshold), whereupon the RLV attempts a circular pullup maneuver. Because the RLV has normal acceleration limits, the flight-path rotation is not successful, and the vehicle hits the ground about 4200 ft short of the runway at a flight-path angle between -18 and -19 deg. Sink rate at impact is between -137 and -156 ft/s, which would clearly result in loss of the vehicle.

Conclusions

A new approach and landing (A&L) guidance method has been developed for an unpowered reusable launch vehicle (RLV) with limited normal acceleration capabilities. The guidance algorithm determines the minimum constant equilibrium-glide load factor such that the flight-path angle is continually increased during the A&L phase. Minimum load factor is determined by numerically propagating A&L trajectories to touchdown and iterating on one parameter (initial flight-path angle) until the acceptable touchdown sink rate is achieved. Once the minimum load factor is determined, the corresponding A&L trajectory is used as the reference path for a closed-loop guidance scheme. Numerical simulations of the closed-loop guidance method show that the RLV is able to achieve the desired touchdown state with a minimum load factor of about $1.1g$

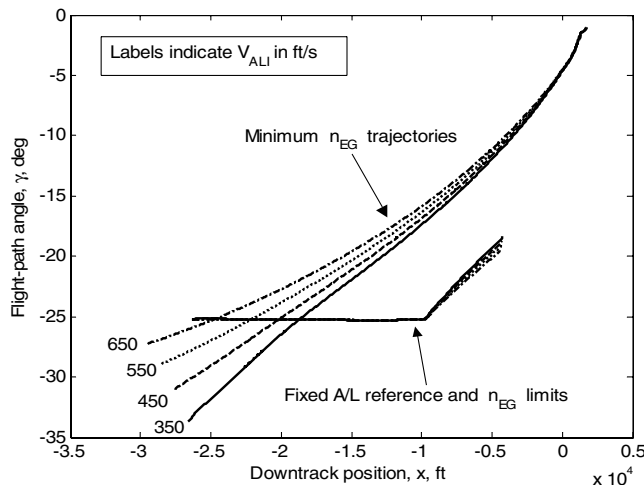


Fig. 1 Flight-path angle vs downtrack position.

for a range of initial energy configurations. These results demonstrate that the proposed guidance method may be a feasible technique for onboard generation of a new reference A&L trajectory.

References

- [1] Hanson, J. M., "A Plan for Advanced Guidance and Control Technology for 2nd Generation Reusable Launch Vehicles," AIAA Paper 02-4557, Aug. 2002.
- [2] Hanson, J. M., "New Guidance for New Launch Vehicles," *Aerospace America*, Vol. 41, No. 3, March 2003, pp. 36–41.
- [3] Hanson, J. M., and Jones, R. E., "Test Results for Entry Guidance Methods for Space Vehicles," *Journal of Guidance, Control, and Dynamics*, Vol. 27, No. 6, 2004, pp. 960–966.
- [4] Calise, A., and Brandt, N., "Generation of Launch Vehicle Abort Trajectories Using a Hybrid Optimization Method," *Journal of Guidance, Control, and Dynamics*, Vol. 27, No. 6, 2004, pp. 930–937.
- [5] Dukeman, G. A., "Profile-Following Entry Guidance Using Linear Quadratic Regulator Theory," AIAA Paper 02-4457, Aug. 2002.
- [6] Zimmerman, C., Dukeman, G., and Hanson, J., "An Automated Method to Compute Orbital Reentry Trajectories with Heating Constraints," AIAA Paper 02-4454, Aug. 2002.
- [7] Shen, Z., and Lu, P., "Dynamic Lateral Entry Guidance Logic," *Journal of Guidance, Control, and Dynamics*, Vol. 27, No. 6, 2004, pp. 949–959.
- [8] Chen, D. T., Saraf, A., Leavitt, J. A., and Mease, K. D., "Performance of Evolved Acceleration Guidance Logic for Entry (EAGLE)," AIAA Paper 02-4456, Aug. 2002.
- [9] Schierman, J. D., Ward, D. G., Hull, J. R., Gandhi, N., Oppenheimer, M. W., and Doman, D. B., "Integrated Adaptive Guidance and Control for Re-Entry Vehicles with Flight-Test Results," *Journal of Guidance, Control, and Dynamics*, Vol. 27, No. 6, 2004, pp. 975–988.
- [10] Kluever, C. A., "Unpowered Approach and Landing Guidance Using Trajectory Planning," *Journal of Guidance, Control, and Dynamics*, Vol. 27, No. 6, 2004, pp. 967–974.
- [11] Tsikalas, G. M., "Space Shuttle Autoland Design," AIAA Paper 82-1604-CP, Aug. 1982.
- [12] Kluever, C. A., and Horneman, K. R., "Terminal Trajectory Planning and Optimization for an Unpowered Reusable Launch Vehicle," AIAA Paper 2005-6058, Aug. 2005.